doi:10.1093/brain/awq171 Brain 2010: 133; 2749–2762 | 2749

BRAIN
A JOURNAL OF NEUROLOGY

Electroclinical characterization of epileptic seizures in leucine-rich, glioma-inactivated 1-deficient mice

Elodie Chabrol,[1] Vincent Navarro,[1,2] Giovanni Provenzano,[1,3] Ivan Cohen,[1] Céline Dinocourt,[1] Sophie Rivaud-Péchoux,[1] Desdemona Fricker,[1] Michel Baulac,[1,2] Richard Miles,[1] Eric LeGuern[1,4] and Stéphanie Baulac[1]

1 CRICM UPMC/INSERM UMR_S975/CNRS UMR7225, Hôpital de la Pitié-Salpêtrière, 75013 Paris, France
2 Epileptology unit, AP-HP, Hôpital de la Pitié-Salpêtrière, 75013 Paris, France
3 Institute of Neurological Sciences, National Research Council, Piano Lago di Mangone, 87050 Cosenza, Italy
4 Département de Génétique et Cytogénétique, AP-HP, Hôpital de la Pitié-Salpêtrière, 75013 Paris, France

Correspondence to: Stéphanie Baulac,
CRICM UMR_S975,
Hôpital de la Pitié-Salpêtrière,
Bâtiment Pharmacie,
47 Bd de l'hôpital,
75013 Paris, France
E-mail: stephanie.baulac@upmc.fr

Mutations of the *LGI1* (*leucine-rich, glioma-inactivated 1*) gene underlie autosomal dominant lateral temporal lobe epilepsy, a focal idiopathic inherited epilepsy syndrome. The *LGI1* gene encodes a protein secreted by neurons, one of the only non-ion channel genes implicated in idiopathic familial epilepsy. While mutations probably result in a loss of function, the role of LGI1 in the pathophysiology of epilepsy remains unclear. Here we generated a germline knockout mouse for LGI1 and examined spontaneous seizure characteristics, changes in threshold for induced seizures and hippocampal pathology. Frequent spontaneous seizures emerged in homozygous LGI1$^{-/-}$ mice during the second postnatal week. Properties of these spontaneous events were examined in a simultaneous video and intracranial electroencephalographic recording. Their mean duration was 120 $\pm$ 12 s, and behavioural correlates consisted of an initial immobility, automatisms, sometimes followed by wild running and tonic and/or clonic movements. Electroencephalographic monitoring indicated that seizures originated earlier in the hippocampus than in the cortex. LGI1$^{-/-}$ mice did not survive beyond postnatal day 20, probably due to seizures and failure to feed. While no major developmental abnormalities were observed, after recurrent seizures we detected neuronal loss, mossy fibre sprouting, astrocyte reactivity and granule cell dispersion in the hippocampus of LGI1$^{-/-}$ mice. In contrast, heterozygous LGI1$^{+/-}$ littermates displayed no spontaneous behavioural epileptic seizures, but auditory stimuli induced seizures at a lower threshold, reflecting the human pathology of sound-triggered seizures in some patients. We conclude that LGI1$^{+/-}$ and LGI1$^{-/-}$ mice may provide useful models for lateral temporal lobe epilepsy, and more generally idiopathic focal epilepsy.

Keywords: autosomal dominant lateral temporal epilepsy; temporal lobe epilepsy; audiogenic; monogenic

Abbreviations: ADAM = postsynaptic disintegrin and metalloproteinase domain; ADLTE = autosomal dominant lateral temporal epilepsy; LGI1 = leucine-rich, glioma-inactivated 1

Received April 5, 2010. Revised May 9, 2010. Accepted May 14, 2010. Advance Access publication July 21, 2010

Introduction

Nearly all mutated genes that have been linked to monogenic idiopathic epilepsies code for components of ion channels or neurotransmitter receptors (Baulac and Baulac, 2009). *Leucine-rich, glioma-inactivated 1* (*LGI1*), along with *Myoclonin1/EFHC1*, is an exception. Mutations in the *LGI1* gene are associated with the autosomal dominant lateral temporal epilepsy (ADLTE) syndrome (Poza *et al.*, 1999), also known as autosomal dominant partial epilepsy with auditory features (Winawer *et al.*, 2000).

ADLTE is an inherited epilepsy syndrome of adolescence onset, characterized by focal seizures that may generalize. A specific feature of the syndrome is the presence of auditory auras. Many patients hear sounds including singing, ringing, humming or whistling during seizures, and seizures may also be triggered by noises or voices. Other less-frequent auras include visual, psychic, autonomic and other feelings or sensations (Michelucci *et al.*, 2009).

Interictal electroencephalography shows temporal abnormalities in 47% of the patients. Magnetic resonance image findings are often normal and outcome is usually good, although some patients may develop pharmacoresistance (Chabrol *et al.*, 2007; Di Bonaventura *et al.*, 2009). While the prevalence of ADLTE is not entirely certain, it may account for up to 19% of familial idiopathic focal epilepsies (Michelucci *et al.*, 2009).

In 2002, mutations responsible for ADLTE were identified in the *LGI1* gene by positional cloning (Kalachikov *et al.*, 2002; Morante-Redolat *et al.*, 2002). A number of ADLTE families and some sporadic cases with mutations in *LGI1* were subsequently reported (Nobile *et al.*, 2009). Nearly half of known ADLTE-related *LGI1* mutations are nonsense and frameshift mutations, some of which are predicted to cause a decreased abundance of mutated mRNA transcripts because of their degradation by nonsense-mediated decay. Other mutations are typically missenses. We and others have shown that missense or truncating mutations impair LGI1 secretion, which also suggests that LGI1-related epilepsy results from a loss of function (Senechal *et al.*, 2005; Sirerol-Piquer *et al.*, 2006; Chabrol *et al.*, 2007; Striano *et al.*, 2008; de Bellescize *et al.*, 2009). It seems likely, therefore, that ADLTE patients carrying nonsense or missense mutations express lower levels of extracellular brain LGI1 protein, causing haploinsufficiency. Two recent articles describing seizures in LGI1-deficient mice confirmed that lack of LGI1 leads to epilepsy (Fukata *et al.*, 2010; Yu *et al.*, 2010).

LGI1 encodes a neuronal protein (also called epitempin) that is secreted into the extracellular media by transfected mammalian cells (Senechal *et al.*, 2005). Expression is highest in the brain (Chernova *et al.*, 1998; Furlan *et al.*, 2006; Head *et al.*, 2007). *LGI1* has no homology with known ion channel genes. Instead, it encodes a protein containing three leucine-rich repeats in the N-terminal half followed by seven epilepsy-associated repeats in the C-terminal part of the protein. Current evidence suggests that LGI1 is a multi-functional protein: (i) it suppresses glial tumour cell progression *in vitro* (Chernova *et al.*, 1998); (ii) it co-purifies with the presynaptic voltage-gated Kv1.1 potassium channel and inhibits fast inactivation of the K^+-currents mediated by the Kvβ1 subunit (Schulte *et al.*, 2006); (iii) LGI1-oligomers bind to postsynaptic disintegrin and metalloproteinase domains 22 and 23 (ADAM22 and ADAM23) (Sagane *et al.*, 2008), and binding to ADAM22 may enhance AMPA receptor-mediated synaptic transmission (Fukata *et al.*, 2006); and (iv) LGI1 also contributes to postnatal dendritic pruning and the maturation of glutamatergic synapses in the hippocampal dentate gyrus (Zhou *et al.*, 2009).

Since mutations may result in *LGI1* haploinsufficiency in patients with ADLTE, we attempted to model the human genetic disorder by disrupting the *LGI1* gene. We found that adult heterozygous mice have reduced seizure thresholds, and homozygous mice display early-life spontaneous seizures associated with neuronal loss in the hippocampus.

Materials and methods

Targeted disruption of the *LGI1* gene

A mouse line harbouring a 'floxed' (*loxP*-flanked encompassing exons 6 and 7) conditional allele of *LGI1* was established at the Mouse Clinical Institute (Illkirch, France). The targeting vector was constructed as follows. A 1.1 kb fragment encompassing *LGI1* exons 6 and 7 was amplified by polymerase chain reaction on 129S2/SvPas mouse embryonic stem cells genomic DNA and subcloned in a Mouse Clinical Institute proprietary vector, resulting in a step 1 plasmid. This Mouse Clinical Institute vector has a floxed neomycin resistance cassette. A 4.4 kb 5′ homologous arm encompassing part of intron 4, exon 5 and part of intron 5 was amplified by polymerase chain reaction and subcloned in step1 plasmid to generate the step2 plasmid and finally a 3.4 kb 3′ homologous arm was subcloned in a step2 plasmid to generate the final targeting construct. The linearized construct was electroporated in 129S2/SvPas mouse embryonic stem cells. After selection, targeted clones were identified by polymerase chain reaction using external primers and further confirmed by Southern blot with 5′ and 3′ external probes. Two positive embryonic stem clones were injected into C57BL/6J blastocystes, and the derived male chimeras gave germline transmission. Crossing $LGI1^{loxP/+}$ males with PGK-Cre females (C57BL/6J) yielded heterozygous $LGI1^{+/-}$ animals. Polymerase chain reaction analysis of DNA extracted from mouse tails with Purelink™ Genomic DNA purification (Invitrogen) revealed a Cre-dependent *LGI1* allele excision. $LGI1^{+/-}$ animals were then intercrossed to obtain $LGI1^{-/-}$, $LGI1^{+/-}$ and $LGI1^{+/+}$ littermates, derived from 75% C57BL/6 and 25% 129S2Sv/pas hybrid background. $LGI1^{+/+}$ (wild-type) mice harbour 2 *LGI1* wild-type alleles (not floxed) and serve as controls. Animals were treated according to the guidelines of the European Community (authorization number 75-1622) and our protocol was approved by the Local Ethical Committee for animal experimentation. All efforts were made to minimize the number of animals and their suffering.

Western blots

Mice were decapitated; whole brains and organs were quickly removed and lysed in 5 M urea, 2.5% sodium dodecyl sulphate, 50 mM Tris, 30 mM NaCl buffer. Total protein concentrations were determined by the Bradford method. Of each sample, 25 μg was separated on 10% Tris–glycine polyacrylamide gels, analysed by Western blot using the following antibodies: rabbit polyclonal anti-LGI1

antibody (ab30868; 1 mg/ml; Abcam), rabbit polyclonal anti-LGI1 antibody (sc-28238 H56; 1 mg/ml; Santa Cruz) and monoclonal anti α-tubulin antibody (1/2000, Sigma Aldrich).

Animal surgery

Under deep peritoneal anaesthesia (ketamine 100 mg/kg and xylazine 10 mg/kg) homozygous, heterozygous and wild-type postnatal day 8 mice (4–5 g) and heterozygous and wild-type postnatal day 21 mice (10–12 g) were implanted with two nickel–chromium epidural electrodes placed symmetrically in the somatosensory cortex (2.5 mm posterior to bregma, 1.84 mm lateral to midline). Two electrodes were placed along the median line, the anterior one as neutral and the posterior one as reference. A nickel–chromium bipolar electrode was placed in the dorsal hippocampus in postnatal day 8 mice (1.7 mm posterior to bregma, 1.8 mm lateral to midline and 1.6 mm ventral).

Intracranial video-EEG recordings

Animals were placed in a round transparent cage in which they were free to move, and were connected to a recording system. EEG signals were amplified with a band-pass filter setting of 0.5–100 Hz with a 24-channel system (Medelec, Oxford Instruments) and digitized at 1024 Hz with a 22-bit resolution. Since postnatal day 9 newborn pups are not weaned, recordings were limited to 4–5 h per day. Animal behaviour and EEG signal were visually inspected.

Audiogenic stimuli

After 1 min of habituation in a Plexiglas box, mice were exposed to a loud acoustic stimulus (11 kHz, 93 dB) generated by a function generator (Wavetek 131A) connected to four loudspeakers. The sound was terminated either when a seizure was triggered or after 80 s (four times 20 s with a 2 s interval between each exposure) as previously (Yagi *et al.*, 2005). Mice were subjected to a single auditory stimulation, and responses were studied by an investigator blind to the genotype of the animal.

Histochemistry

Mice aged postnatal day 8 and postnatal day 14 were deeply anaesthetized with sodium pentobarbital (50 mg/kg by intraperitoneal injection) and then perfused with 4% paraformaldehyde in a 0.1 mol/l phosphate buffer, pH 7.4. Brains were removed, postfixed in the same fixative for 2 h at 4°C, cryoprotected for 24 h in a 30% sucrose solution, frozen in isopentane (−30°C) and stored at −80°C. Immunohistochemistry was performed using 20 µm free-floating sections. For all experiments, a series of three littermate mice corresponding to each genotype were processed simultaneously. Antibodies used were rabbit polyclonal antibody against ZnT3 (1:500; kindly provided by R. Palmiter), rabbit polyclonal antibody against glial fibrillary acidic protein (1:4000; Dako) and biotinylated secondary antibody (Vector Laboratories). A Nissl counterstaining (0.8% cresyl violet) was done to reveal neuronal cytoarchitecture. Brain slices were labelled with Fluoro-Jade C according to manufacturer's instructions (Histo-Chem Inc.).

Statistical analysis

Mendelian and sex ratios were assessed by using the χ^2-test. For the body-weight plot, we have compared weight ratios between two timepoints rather than absolute values in order to avoid variability of body weight at birth between independent litters. A Kruskal–Wallis test was used to compare body weight evolution of the three genotypes (68 pups from 7 litters). Subsequently, we performed a Mann–Whitney test to compare LGI1$^{-/-}$ mice to LGI1$^{+/-}$ and wild-type mice. The thickness of the granule cell layer was measured in three brain sections from three mice of each genotype. Means were compared using a Mann–Whitney test.

Results

Generation of LGI1-deficient mice

We targeted the *LGI1* gene in murine embryonic stem cells by homologous recombination with a conditional Cre-*LoxP* approach. *LGI1*$^{loxP/+}$ mice with a floxed *LGI1* conditional allele were produced in a 75% C57BL/6, 25% 129S2Sv/pas hybrid line. *LGI1*$^{loxP/+}$ males were crossed with *PGK*-Cre females (C57BL/6), which express the Cre recombinase early and ubiquitously under the control of the phosphoglycerate kinase 1 (*PGK*) promoter. Recombination was observed in all organs due to maternal transmission of active Cre recombinase in the oocyte (Lallemand *et al.*, 1998), leading to the deletion of exons 6 and 7 with a frameshift generating a premature stop codon at residue 179 of the protein (Fig. 1A).

Breeding pairs of adult heterozygous LGI1$^{+/-}$ yielded litters with wild-type ($^{+/+}$), heterozygous ($^{+/-}$) and homozygous ($^{-/-}$) genotypes born in Mendelian ratios. Of 472 mice born, 120 were LGI1$^{+/+}$, 248 were LGI1$^{+/-}$ and 104 were LGI1$^{-/-}$ as predicted by Mendelian transmission ($\chi^2 = 2.3$, nonsignificant), suggesting that loss of both *LGI1* alleles during embryogenesis is not lethal. Sex ratios in LGI1$^{-/-}$ mice were approximately 1 : 1 (107 females, 123 males; $\chi^2 = 1.1$, nonsignificant) as expected.

LGI1 protein expression was examined by Western blot of whole brain lysates from LGI1$^{-/-}$, LGI1$^{+/-}$ and wild-type littermate mice. Immunoblot with an antibody against residues 200–300 of LGI1 (ab30868) revealed a single band of 65 kDa. The intensity of the band was reduced by about half in LGI1$^{+/-}$ lysate and the band was absent in LGI1$^{-/-}$, confirming that the full-length LGI1 protein was completely ablated (Fig. 1B). A second LGI1 antibody (sc-28238) directed against the N-terminus (amino acids 35–90) detected the full-length protein, but not a lower band, suggesting that a putative truncated protein (179 amino acids) was absent (Fig. 1C). Neither antibody cross-reacted with other LGI subfamily proteins, whereas a commercial anti-LGI1 antibody (sc-9581, N18) directed against the N-terminal region may do so (S. Baulac, personal communication). We also examined the developmental and tissue expression pattern of LGI1 using the specific ab30868 antibody. LGI1 expression could be detected at low levels as early as embryonic day 16 and increased with age, reaching plateau levels in the adult (Fig. 1D). LGI1 expression was only detected in mouse brain and spinal cord extracts (Fig. 1E).

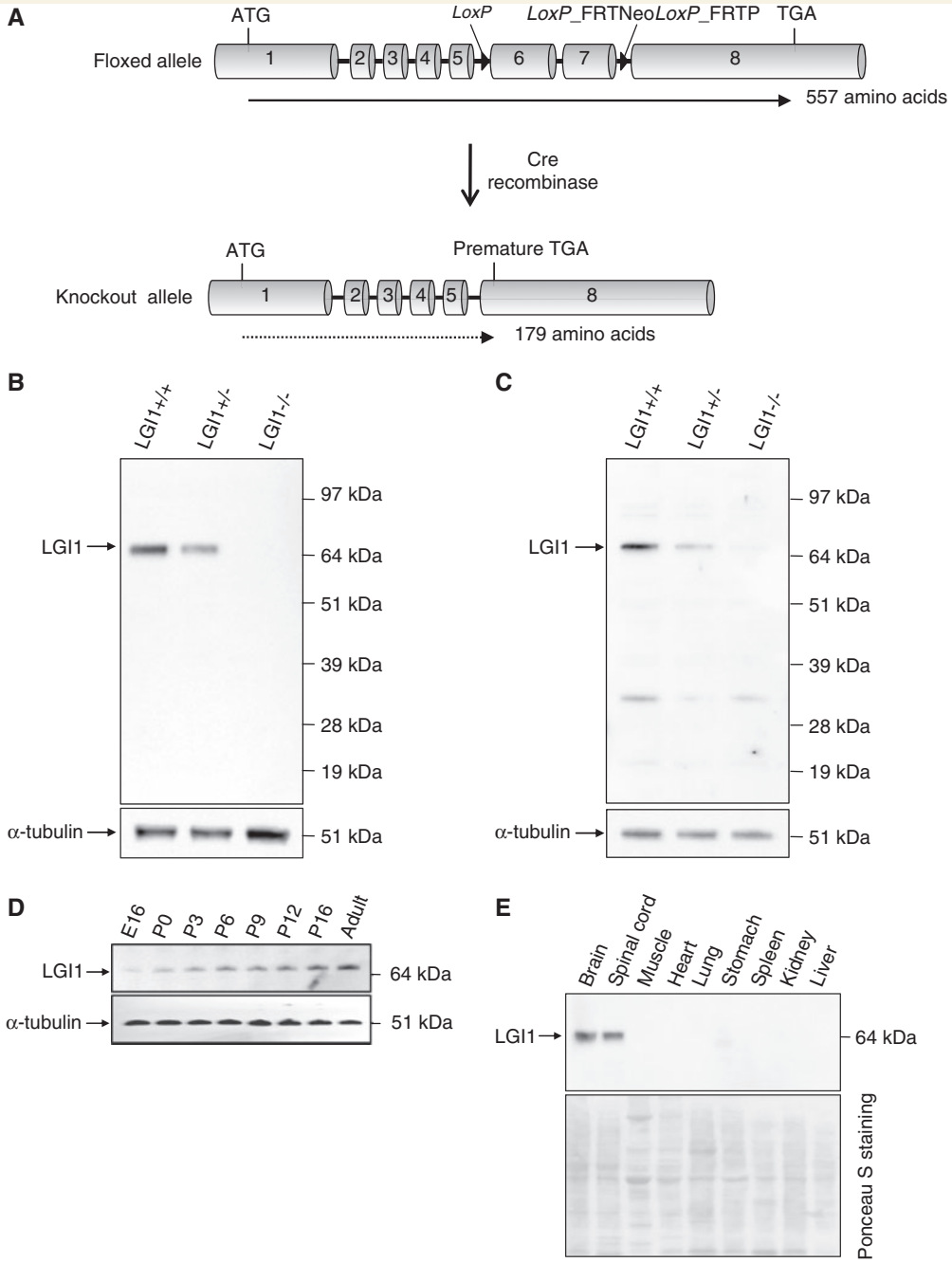

Figure 1 Generation of the *LGI1* knockout mouse. (**A**) Diagram showing *LoxP* and *LoxP*-Neo-*LoxP* sequences indicated by triangles (floxed allele). Exons 6 and 7 were removed by crossing the LGI1^{loxP} mice with a PGK-Cre strain (knockout allele). (**B–C**) Western blots demonstrating the absence of native LGI1 protein in whole brain lysate of LGI1$^{-/-}$ mouse (at postnatal day 13) using the ab30868 antibody (**B**), and spinal cord lysate of LGI1$^{-/-}$ mouse using the sc-28238 antibody (**C**). Equal amounts of total protein were loaded as demonstrated by α-tubulin levels. (**D**) Western blot showing LGI1 expression during embryonic and postnatal development on C57BL/6 mouse brain lysate (ab30868) and α-tubulin used for internal control. (**E**) Western blot showing restricted expression of LGI1 in the brain and spinal cord of a postnatal day 15 wild-type mouse (ab30868). Equal amounts of total protein were loaded and Ponceau S staining was used as internal loading control.

Homozygous LGI1$^{-/-}$ mice display early onset spontaneous seizures

The behaviour and appearance of LGI1$^{-/-}$ mice at birth did not differ from that of LGI1$^{+/-}$ and wild-type littermates. In the second postnatal week, however, both male and female LGI1$^{-/-}$ mice began to exhibit frequent spontaneous seizures. Seizures were first observed at postnatal day 10, especially during cage changing and handling. They consisted of a behavioural sequence including (i) movement arrest, sometimes associated with limb

jerks; (ii) hyperkinetic running, often with repeated, large clonics of all limbs and frequently incontinence and loss of postural equilibrium; and (iii) dystonic or hypertonic posture of the trunk, limbs and tail, often asymmetrically. Motor automatisms such as chewing and grooming also occurred and some mice exhibited four-limb tonic–clonic seizures (Fig. 2; Supplementary material movie). Seizures often ended after hypertonic postures. Mice were immobile for 2–3 min and sometimes catatonic after seizures. At postnatal day 14, LGI1$^{-/-}$ mice became inactive, except during seizures, and usually remained isolated in their cage. Heterozygous LGI1$^{+/-}$ and wild-type littermates never showed spontaneous epileptic manifestations.

Video-EEG recording demonstrates epileptic activity in LGI1$^{-/-}$ mice

Spontaneous seizures in LGI1$^{-/-}$ mice were studied in simultaneous video and intracranial EEG recordings from postnatal days 10–15 pups. Ictal epileptic EEG abnormalities were evident in all homozygous LGI1$^{-/-}$ mice ($n = 6$), and 52 spontaneous electroclinical seizures were recorded (Fig. 3A). Epileptic activity was never detected in age-matched heterozygous LGI1$^{+/-}$ ($n = 5$) (Fig. 3B) or wild-type ($n = 5$) (Fig. 3C) littermates. Cortical EEG records from LGI1$^{-/-}$ pups ($n = 6$) revealed sequences of several ictal electrographic patterns: (i) low amplitude fast activities (18–47 Hz); (ii) bursts or discharges of polyspikes of increasing amplitude and decreasing frequency (20–27 Hz) and (iii) high amplitude slow potentials, close to 1 Hz, with superimposed low-voltage polyspikes (Fig. 3A). Ictal EEG activities were often bilateral, but asymmetrical seizure terminations suggestive of partial seizures were sometimes detected (Fig. 3D).

In three LGI1$^{-/-}$ pups, EEG signals were recorded from both cortex and hippocampus (Fig. 4). Periods of physiological theta rhythm were evident in the hippocampal EEG between seizures (Fig. 4E). During seizures, ictal electrographic activities were recorded concomitantly in the cortex and hippocampus. Our data suggest that seizures may be initiated in the hippocampus. They were often preceded by a sharp wave or a spike and wave, of larger amplitude in the hippocampus than in the cortex. Further, seizures appeared to be initiated with low voltage fast activities that started 1–2 s earlier in the hippocampus than in the cortex (Fig. 4A). After prolonged seizures, EEG activity was profoundly depressed (Fig. 4D) until interictal activity reappeared after a few minutes. Interictal activities consisted of spikes, polyspikes, spikes and waves and were more abundant in the hippocampus (Fig. 4C). Brief ictal EEG discharges with no obvious behavioural counterpart were also observed after the first seizures between

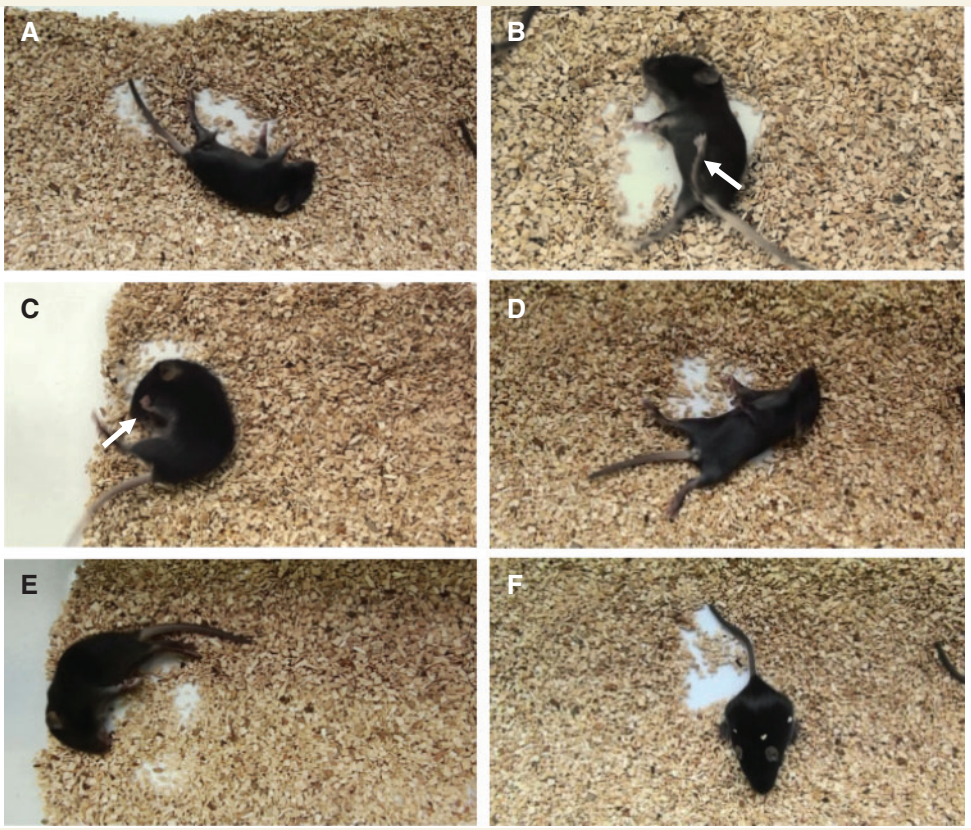

Figure 2 Spontaneous seizures in homozygous LGI1$^{-/-}$ mice**.** Frames from a video recording of a spontaneous seizure in a postnatal day 16 LGI1$^{-/-}$ mouse. (**A**) Onset of the seizure with forelimb and hind limb flexion and loss of postural equilibrium, (**B**) asymmetrical tonic extension (arrow) with rigidity of the tail, (**C**) chewing mechanism (arrow), (**D**) beginning of the hypertonic phase, (**E**) hypertonic phase with characteristic rigid hind limb extension and (**F**) postictal immobility. The behavioural seizure lasted for 100 s.

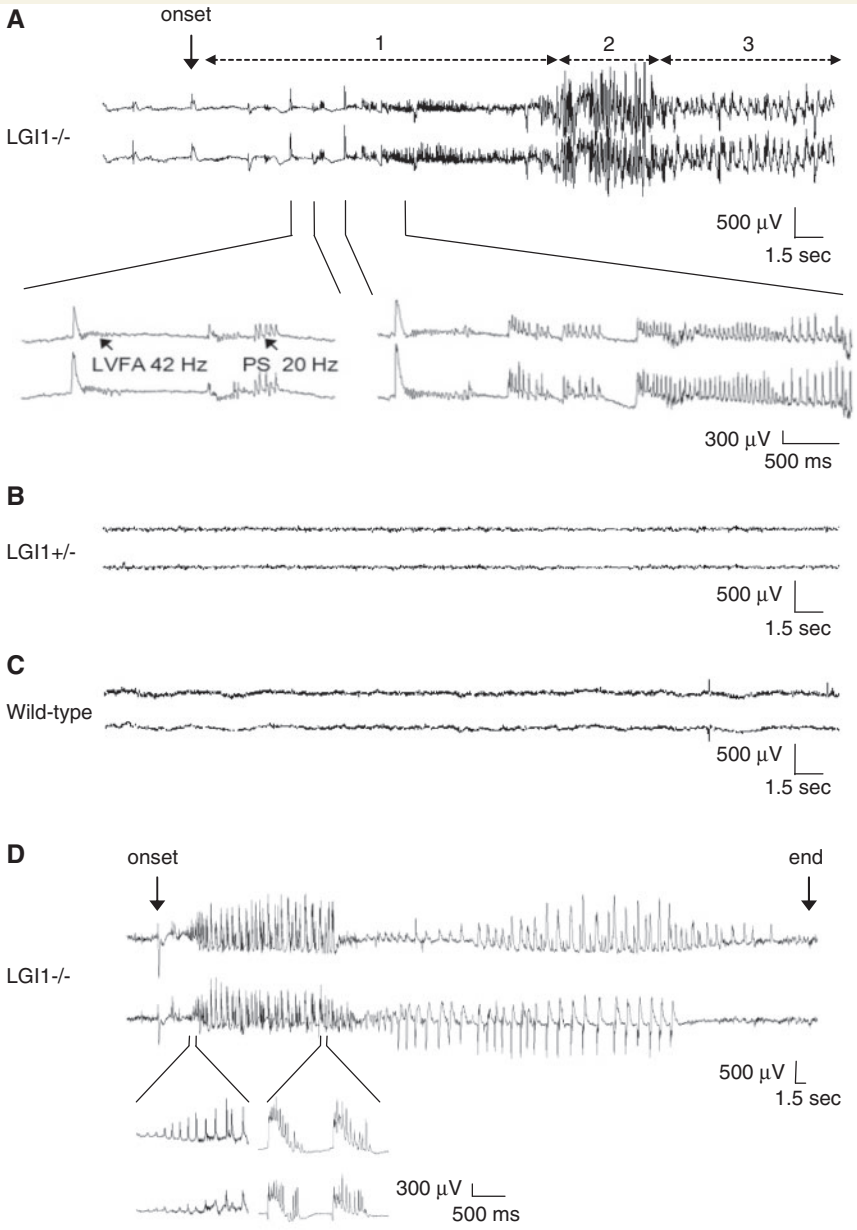

Figure 3 Video–EEG recordings of LGI1$^{-/-}$, LGI1$^{+/-}$ and wild-type mice. (**A**) Epidural EEG recording in a postnatal day 10 LGI1$^{-/-}$ mouse showing the onset of an electroclinical seizure (upper trace corresponds to the right cortex and bottom trace to the left cortex). Behavioural modifications were correlated with EEG changes: 1 = immobility; 2 = repeated clonies of the four limbs, agitation; 3 = myoclonic jerks of the trunk. In the lower panel, expanded EEG traces show low voltage fast activities (LVFA) following spikes, and bursts of polyspikes (PS) with increasing duration. No EEG abnormality was seen in age-matched LGI1$^{+/-}$ (**B**) or wild-type (**C**) mice. (**D**) Epidural EEG recording in a postnatal day 10 LGI1$^{-/-}$ mouse. In the lower panel, expanded EEG traces show initial spikes discharge with increasing amplitude, and then pseudo-periodic slow potentials with over-imposed polyspike activity. Note the asymmetry at the end of the seizure.

postnatal days 11 and 15, within the cortex and/or hippocampus (Fig. 4B).

The percentage of mice showing electroclinical seizures reached a peak at postnatal day 10, and then a second peak at postnatal day 14 (Fig. 4F). Neither the frequency nor the duration of electroclinical seizures changed appreciably with age. Seizure frequency fluctuated with a mean frequency of 1.6 ± 0.6 ictal events per hour at postnatal day 14 (Fig. 4F). The mean duration of seizures for animals over all recorded ages was 120 ± 12 s (Fig. 4G).

Homozygous LGI1$^{-/-}$ mice die prematurely

All homozygous LGI1$^{-/-}$ mice died prematurely, and Kaplan–Meier curves revealed a mean lifetime of 16 days (n = 25; SD = 1.8).

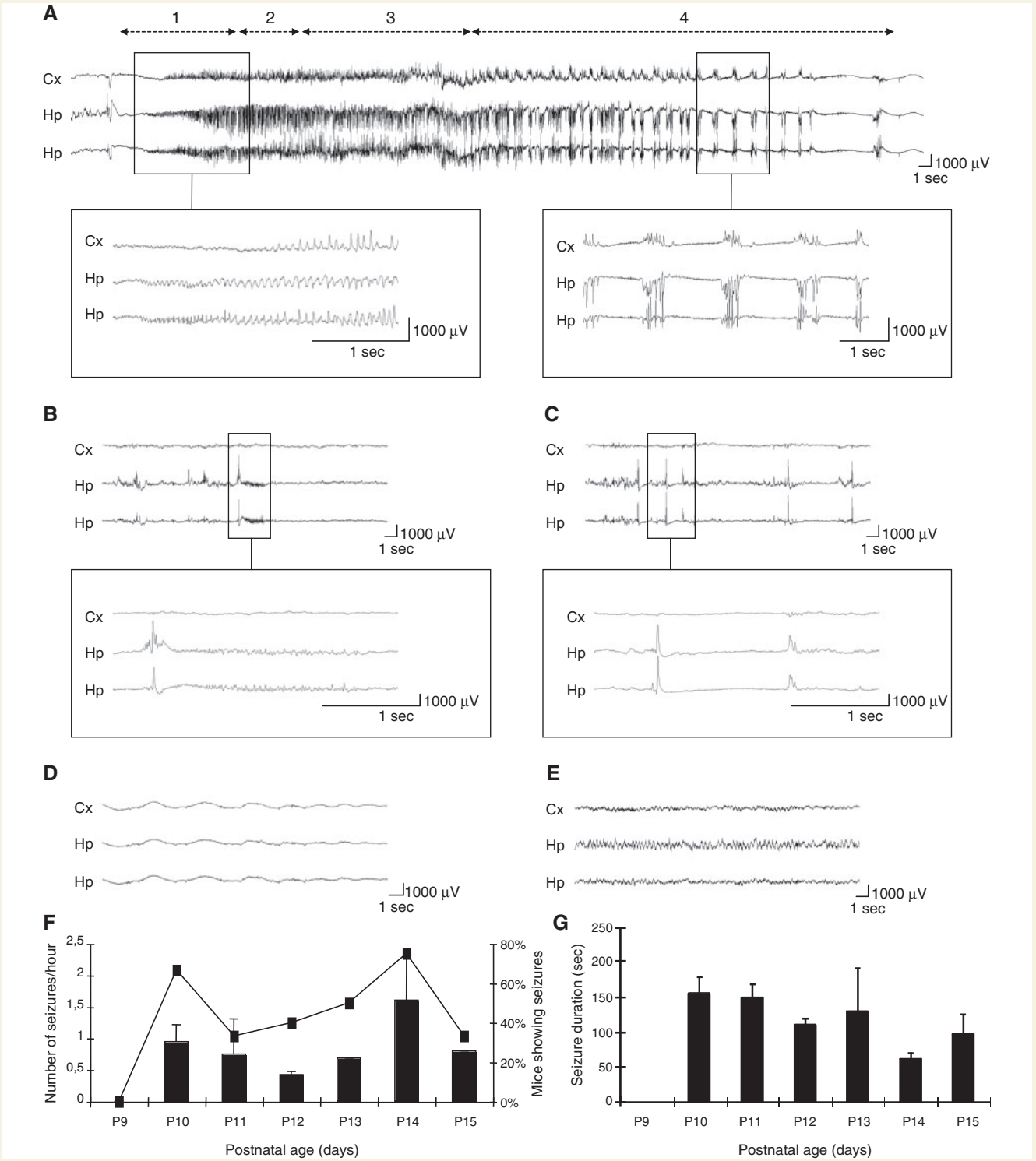

Figure 4 Simultaneous video–EEG recordings of the cortex and the hippocampus in homozygous LGI1$^{-/-}$ mice. (**A**) Two electrodes located in the dorsal hippocampus (Hp) and one in the adjacent cortex (Cx) record an electroclinical seizure. Behavioural modifications are correlated with EEG event: 1 = immobility; 2 = myoclonic jerks; 3 = agitation and wild running; 4 = four-limb hypertonia. In the lower panel, an expanded EEG trace shows initial spike discharges of increasing amplitude, which begin earlier in the hippocampus than in the cortex and then pseudo-periodic slow potentials with an imposed polyspike activity. (**B**) Brief electrical seizure, with no clinical correlate. In this example, which was limited to the hippocampus, polyspikes, resembling interictal activity followed a low voltage fast activity of duration 2 s (see the lower panel for magnification). (**C**) Interictal activity, restricted to the hippocampus, showing high-amplitude spikes and polyspikes. This activity is increased after electroclinical seizures. (**D**) Postictal delta slow waves and depression of the activity at the end of an electroclinical seizure. (**E**) Physiological theta rhythm, with maximum amplitude in the hippocampus. (**F** and **G**) EEG analysis of 52 spontaneous electroclinical seizures recorded in LGI1$^{-/-}$ mice ($n = 6$). (**F**) Percentage of mice showing seizures from postnatal days 9–15 during recordings (curve; axis on the right) and seizure frequency (histogram; axis on the left). (**G**) Seizure duration. Means and SEM are indicated.

No LGI1-null mice survived beyond postnatal day 21 (Fig. 5A), while no LGI1$^{+/-}$ or wild-type littermates had died at this age. We noted at postnatal day 14 that the body weight of LGI1$^{-/-}$ mice was significantly less than that of LGI1$^{+/-}$ ($P = 0.0012$) or wild-type ($P = 0.027$) mice, whereas the body weight at postnatal day 10 was similar for LGI1$^{-/-}$, LGI1$^{+/-}$ or wild-type mice (Fig. 5B). The failure to thrive between postnatal days 10 and 14 was associated with a smaller size (LGI1$^{-/-}$ mice were up to 50% smaller that wild-type littermates) and an apparently slower development in some pups (Fig. 5C). Postmortem examination of LGI1$^{-/-}$ mice at postnatal day 14 revealed an absence of stomach contents (Fig. 5D) and a lack of body fat. While early mortality might result from dehydration and/or starvation due to a failure to feed, we observed that death occurred during prolonged hypertonic episodes in 28% of LGI1$^{-/-}$ mice (at age postnatal days 14, 16 and 17). It may occur even more frequently in unobserved mice. Some pups of smaller litters were moderately malnourished but still died prematurely, suggesting that seizures may have caused their death. One animal died at postnatal day 15 during a prolonged video–EEG recording of more than 4 h with no seizure. Brain activity was progressively reduced during the recording.

Adult heterozygous LGI1$^{+/-}$ mice have lowered threshold to audiogenic seizures

Heterozygous LGI1$^{+/-}$ mice genetically mimic patients with ADLTE. The mice are fertile, behaviourally similar to wild-type animals and live for at least 18 months. Spontaneous clinical seizures have never been observed either in pups or adult mice. Since seizures in patients with ADLTE can be triggered by sound, we examined the susceptibility of LGI1$^{+/-}$ mice to a single sound stimulus at frequency 11 kHz and intensity 93 dB. This stimulus did not induce seizures in LGI1$^{-/-}$, LGI1$^{+/-}$ or wild-type mice at postnatal day 10 (data not shown). At postnatal day 21, some mice exhibited sound-induced seizures, but seizure thresholds of LGI1$^{+/-}$ (seizures induced in 13% of animals) and wild-type mice (seizures induced in 5% of animals tested) were not significantly different (Fig. 6A). In contrast, at age postnatal day 28, auditory stimulation induced seizures in a significantly higher percentage of LGI1$^{+/-}$ than wild-type littermates (52% versus 18%, $P < 0.03$) (Fig. 6A). Typically, audiogenic seizures began suddenly at 5–20 s after the onset of the tone, with wild running, followed by a tonic phase and sudden death in 23% of mice. We examined the cortical EEG of postnatal day 28 LGI1$^{+/-}$ mice ($n = 8$) and wild-type mice ($n = 3$) during auditory stimuli. Cortical electrodes detected no epileptic activity during the wild running or tonic phase (Fig. 6B). Possibly audiogenic seizures are initiated in the brainstem rather than the cortex as previously suggested (Seyfried *et al.*, 1999). The neuronal network of audiogenic seizures remain to be investigated with additional recordings of midbrain structures.

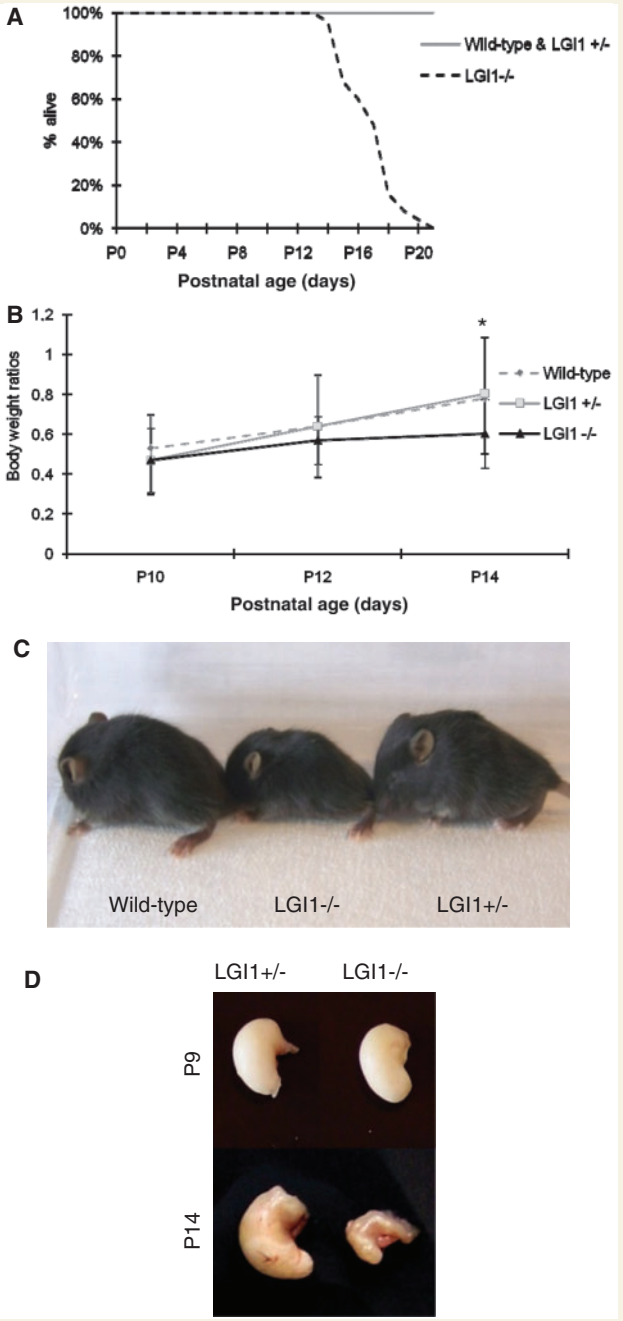

Figure 5 Premature death and reduced body weight in homozygous LGI1$^{-/-}$ mice. (**A**) Kaplan–Meier survival curves of LGI1$^{-/-}$ ($n = 25$), LGI1$^{+/-}$ ($n = 52$) and wild-type ($n = 23$) mice from postnatal day 0 until postnatal day 20. Of the LGI1$^{-/-}$ mice 50% had died at postnatal day 17. (**B**) Body weight was comparable for LGI1$^{-/-}$ ($n = 21$), LGI1$^{+/-}$ ($n = 27$) and wild-type ($n = 20$) animals between postnatal days 8 and 10. Between postnatal days 8 and 14, the body-weight ratio of LGI1$^{-/-}$ mice was reduced with respect to LGI1$^{+/-}$ and wild-type mice. *$P < 0.05$. (**C**) LGI1$^{-/-}$ mice were smaller than LGI1$^{+/-}$ and wild-type littermates at postnatal day 14. (**D**) Stomach content of LGI1$^{-/-}$ mice (empty) and LGI1$^{+/-}$ mice (full) at postnatal day 14. At P9, stomach sizes and contents of LGI1$^{-/-}$ and LGI1$^{+/-}$ mice were similar.

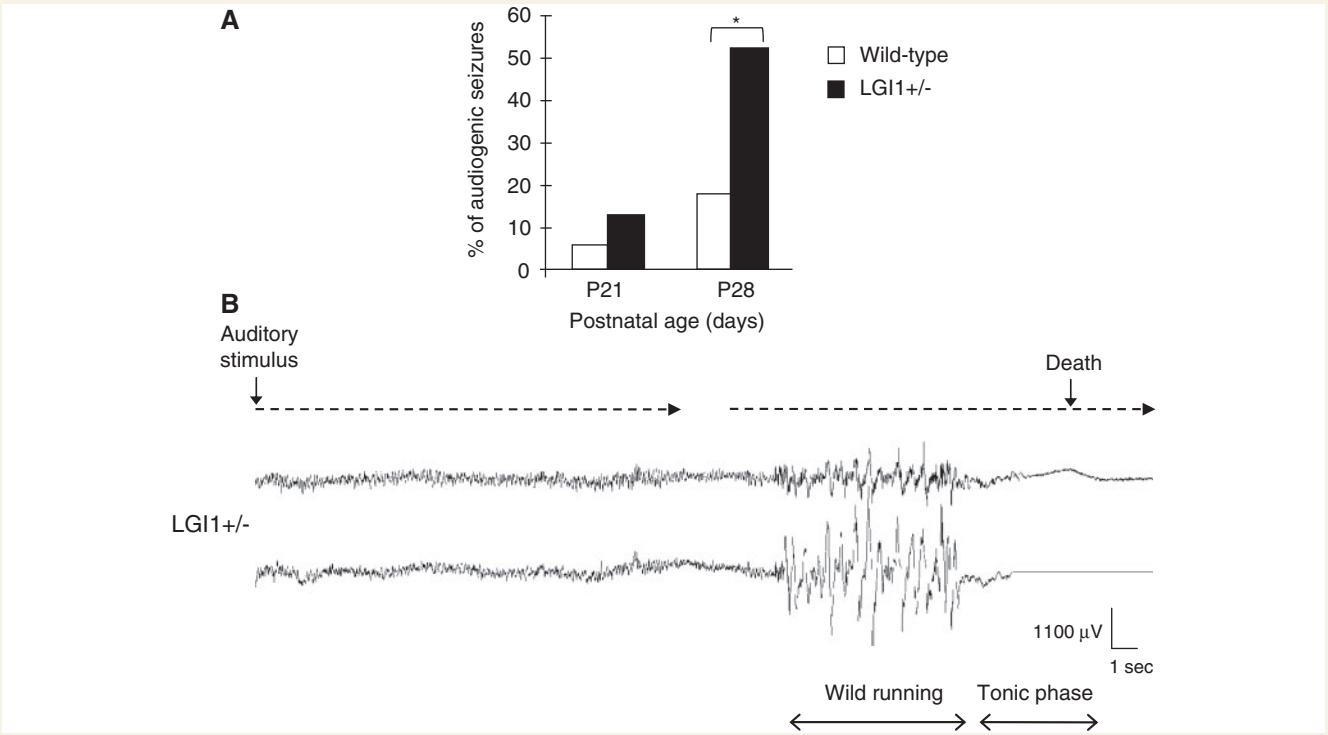

Figure 6 Lower threshold for audiogenic seizures in heterozygous LGI1$^{+/-}$ mice. (**A**) Variation with age in susceptibility to audiogenic seizures of LGI1$^{+/-}$ mice exposed to a sound stimulus (11 kHz, 95 dB) compared with wild-type littermates. At postnatal Day 21, susceptibility was low, while at postnatal day 28, LGI1$^{+/-}$ mice exhibit a significant susceptibility to audiogenic seizures compared with wild-type. *$P < 0.05$. LGI1$^{+/-}$ ($n = 25$), wild-type ($n = 17$). (**B**) Epidural EEG recording in a P28 LGI1$^{+/-}$ mouse under auditory stimulation. During the auditory stimulation (dashed arrow), the mouse was immobile and the EEG showed a normal background activity. Later, the mouse exhibited wild running (associated with movement artifacts), followed by a tonic phase and death (associated with suppression of brain activity).

Seizure-induced brain damage in homozygous LGI1$^{-/-}$ mice

No major differences in cortical or hippocampal organization were evident in Nissl-stained sections prepared before seizure onset at postnatal day 8 (Fig. 7A–C) or after repeated seizures at postnatal day 14 (Fig. 7D–F) in LGI1$^{-/-}$ mice ($n = 4$ for each age) and either LGI1$^{+/-}$ ($n = 4$ for each age) or wild-type ($n = 4$ for each age) animals. Cortical lamination was similar, suggesting that the absence of LGI1 did not affect radial migration of pyramidal cells. However, at postnatal day 14 we detected an abnormal dispersion of dentate granule cells in LGI1$^{-/-}$ mice (Fig. 8C). No such dispersion was evident in wild-type (Fig. 8A), LGI1$^{+/-}$ littermates (Fig. 8B) or in LGI1$^{-/-}$ mice before seizure onset at postnatal day 8 (Fig. 9A). Granule cell layer thickness was significantly increased in LGI1$^{-/-}$ mice compared with LGI1$^{+/-}$ ($P < 3.3E{-}06$) and wild-type ($P < 9.9E{-}05$) mice. Granule cell dispersion is associated with temporal lobe epilepsy in the human and in experimental models. We next investigated other markers of epileptogenesis. We assessed expression of glial fibrillary acidic protein to determine the reactive state of astrocytes in LGI1$^{-/-}$, LGI1$^{+/-}$ and wild-type mice. There was no difference in glial fibrillary acidic protein staining of tissue from LGI1$^{-/-}$ ($n = 3$, Fig. 9F), LGI1$^{+/-}$ ($n = 3$, Fig. 9E) and wild-type ($n = 3$, Fig. 9D) postnatal day 8 pups. In contrast, in LGI1$^{-/-}$ ($n = 3$) animals at P14 after repeated seizures, glial fibrillary acidic protein immunoreactivity increased, particularly in the hilus of the dentate gyrus (Fig. 8F, I), while there was no change in LGI1$^{+/-}$ ($n = 3$) (Fig. 8E, H) or wild-type mice ($n = 3$) (Fig. 8D, G). In temporal lobe epilepsies, mossy fibres often sprout to form aberrant recurrent synapses with dentate granule cells. We used immunostaining against the zinc transporter 3, present at high levels in mossy fibres to label synapses (Palmiter *et al.*, 1996). We consistently detected zinc transporter 3 labelling in the inner molecular layer of the dentate gyrus of LGI1$^{-/-}$ mice after seizures (postnatal day 14), indicating the presence of aberrant mossy fibre terminals ($n = 4$; Fig. 8L, O). In contrast, no zinc transporter 3 labelling was detected in this area in LGI1$^{+/-}$ mice ($n = 4$, Fig. 8K, N) or wild-type mice ($n = 4$, Fig. 8J, M), or in any mouse studied at postnatal day 8 (LGI1$^{-/-}$, $n = 4$; LGI1$^{+/-}$, $n = 4$; wild-type, $n = 4$; Fig. 9G–I). Finally, we asked whether recurrent seizures caused hippocampal neuronal loss in LGI1$^{-/-}$ mice. We used Fluoro-Jade C, which is specific for degenerating neurons (Schmued *et al.*, 2005). After several seizures, Fluoro-Jade C labelling revealed a strong neuronal loss in the CA3 region and a lesser cell death in the CA1 region of LGI1$^{-/-}$ mice aged postnatal day 14 ($n = 3$, Fig. 8P-R), but not in LGI1$^{+/-}$ or wild-type or postnatal day 8 LGI1$^{-/-}$ mice (not shown). We note that the number of Fluoro-Jade C-positive

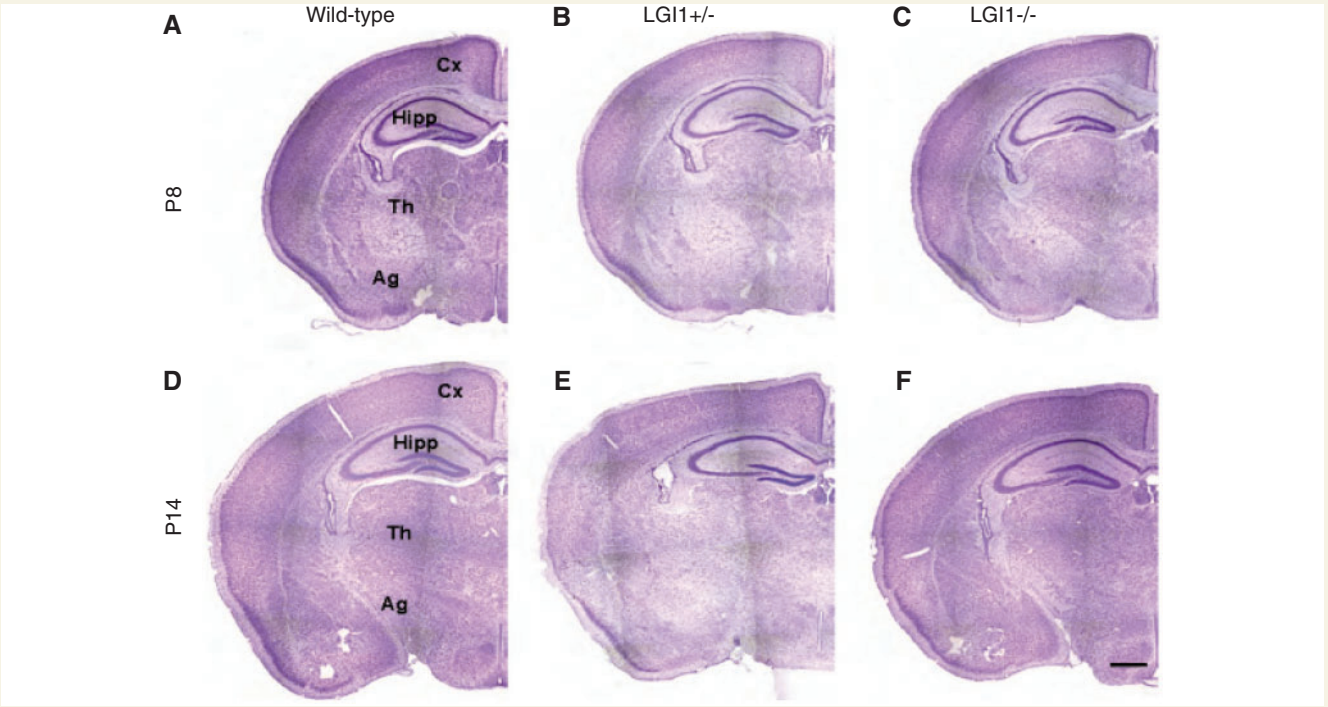

Figure 7 Brain morphology of LGI1$^{-/-}$ mice. (**A–C**) at postnatal day 8 and (**D–F**) at postnatal day 14 (P14). Nissl-stained coronal brain sections show similar brain morphology in (**A** and **D**) wild-type ($n = 3$), (**B** and **E**) LGI1$^{+/-}$ ($n = 3$) and (**C** and **F**) LGI1$^{-/-}$ mice ($n = 3$). Scale bars: 650 μm. Cx = cortex; Hipp = hippocampus; Th = thalamus; Ag = amygdala.

neurons varied among LGI1$^{-/-}$ mice, highlighting the importance of seizure number and severity in neuronal degeneration.

Discussion

We report the electroclinical characterization of seizures in mice deficient for *LGI1*, the gene responsible for ADLTE. Two other reports of LGI1 knockout mice, focusing mainly on *in vitro* dysfunction, have been published recently (Fukata *et al.*, 2010; Yu *et al.*, 2010). Our results also demonstrate early onset spontaneous seizures with premature death in homozygous LGI1$^{-/-}$ mice and an absence of spontaneous seizures in heterozygous LGI1$^{+/-}$ mice. We have further characterized the phenotype of *LGI1*-deficient mice, showing (i) spontaneous epileptic activities with video–EEG monitoring and providing details of seizure semiology; (ii) seizure-induced hippocampal cell death and synaptic rearrangement consistent with a temporal origin for ictal activity and (iii) evidence that heterozygous LGI1$^{+/-}$ mice have lowered threshold to audiogenic seizures, reminiscent of human data for seizures triggered by sound in some patients from ADLTE families.

Homozygous LGI1$^{-/-}$ mice: a model for temporal lobe epilepsy?

Homozygous LGI1$^{-/-}$ mice were born in Mendelian ratios and were undistinguishable from the LGI1$^{+/-}$ and wild-type littermates until age postnatal day 10. At that time, LGI1$^{-/-}$ mice began to display spontaneous seizures that are lethal around postnatal day 16. Video–EEG studies on LGI1$^{-/-}$ mice confirmed that acute behavioural manifestations were associated with epileptic activities, both in the cortex and in the hippocampus. Since seizures in LGI1$^{-/-}$ animals were frequently initiated by behavioural immobility, EEG records were crucial to define seizure occurrence and duration. Initial seizures could be limited to motor arrest, followed by grooming behaviours including forelimb licking (not shown). Succeeding seizures tended to terminate with wild running and tonic–clonic movements. It seems likely that seizures spread to motor areas only at seizure termination. In the absence of EEG records, Yu *et al.* (2010) and Fukata *et al.* (2010), who reported generalized myoclonic seizure and generalized seizures, respectively, may have missed initial ictal symptoms.

Which brain regions underlie seizure initiation in LGI1$^{-/-}$ mice? Our data suggest that spontaneous seizures may have a focal onset reminiscent of complex partial seizures originating in the human temporal lobe. The behaviour during seizures suggests a sequential involvement of different brain areas as expected for propagating epileptic discharges. Initial behaviour included motor arrest and oroalimentary automatisms (forelimb licking, chewing). Dystonic or tonic postures, frequently asymmetrical, tended to involve the four limbs separately toward the end of seizures. The organization of hippocampal EEG activity during seizures, with initial low voltage fast activities followed by spike discharges structured in amplitude and frequency, is similar to intracranial EEG records of human temporal lobe seizures (Navarro *et al.*, 2002). Furthermore, ictal epileptic activities in the hippocampus of LGI1$^{-/-}$ mice tended to precede cortical discharges, suggesting that as in patients with ADLTE, seizures in mice originate focally in

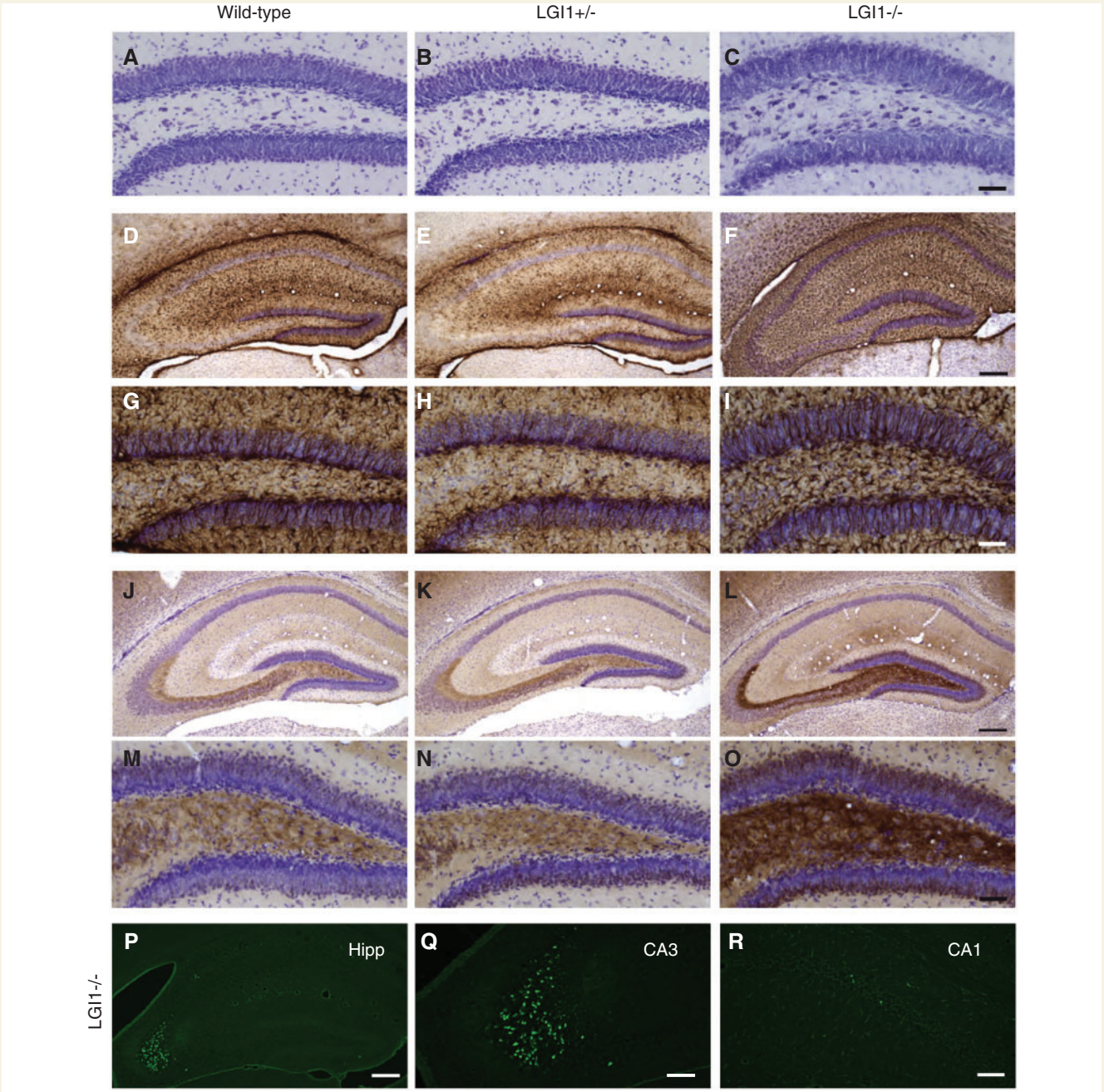

Figure 8 Seizure-induced hippocampal damage in homozygous LGI1$^{-/-}$ mice aged postnatal day 14. (**A–C**) Nissl-staining shows dentate granule cell dispersion in LGI1$^{-/-}$ mice (**C**). (**D–I**) Glial fibrillary acidic protein immunostaining with cresyl violet counterstaining of the hippocampus of (**D**) wild-type ($n = 3$), (**E**) LGI1$^{+/-}$ ($n = 3$) and (**F**) LGI1$^{-/-}$ ($n = 3$) mice. Enlarged images of the dentate gyrus in (**G**) wild-type, (**H**) LGI1$^{+/-}$ and (**I**) LGI1$^{-/-}$ mice. Reactive astrocytes are observed in LGI1$^{-/-}$ mice (**F** and **I**). (**J–O**) Zinc transporter 3 (ZnT3) immunostaining with cresyl violet counterstaining of the hippocampus of (**J**) wild-type ($n = 5$), (**K**) LGI1$^{+/-}$ ($n = 4$) and (**L**) LGI1$^{-/-}$ ($n = 5$) mice. Enlarged images of the dentate gyrus from (**M**) wild-type, (**N**) LGI1$^{+/-}$ and (**O**) LGI1$^{-/-}$ mice showing mossy fibre sprouting in the inner molecular layer of the dentate gyrus of LGI1$^{-/-}$ mice (**L**, **O**). (**P–R**) Fluoro-Jade C positive neurons in the hippocampus (**P**), CA3 region (**Q**) and CA1 region (**R**) of LGI1$^{-/-}$ mice. Scale bars: 160 μm (**D–F**, **J–L**); 60 μm (**A–C**, **G–I**, **M–R**). Hipp = hippocampus.

the temporal structures. We note that some patients with ADLTE describe psychic ('*déjà-vu*') and autonomous symptoms (epigastric sensations), characteristic of mesial temporal lobe auras (Morante-Redolat *et al.*, 2002; Winawer *et al.*, 2002; Ottman *et al.*, 2004).

Further evidence for hippocampal involvement for seizures in LGI1$^{-/-}$ mice was provided by anatomical changes occurring after the onset of recurring ictal events. These changes, which include neuronal cell death, astrocyte reactivity, granule cell dispersion and aberrant mossy fibre sprouting in the dentate gyrus,

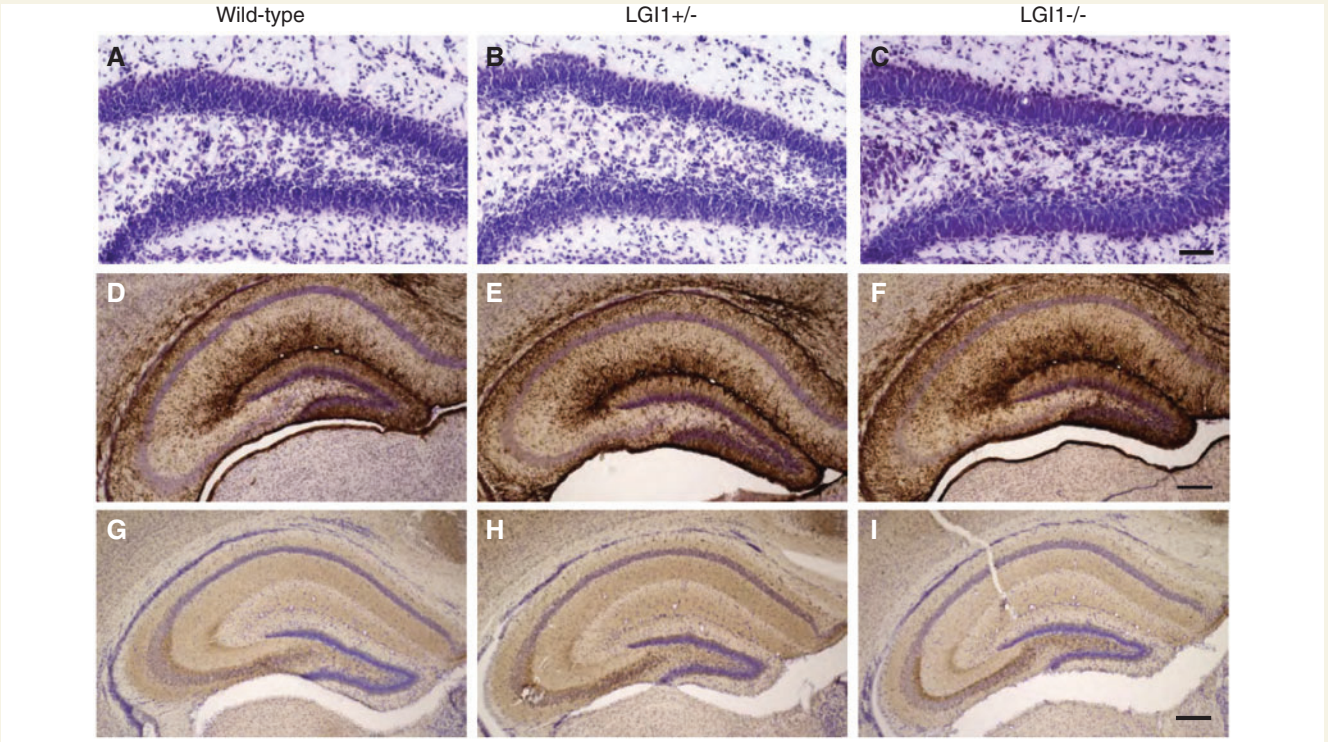

Figure 9 Absence of morphological alterations in LGI1$^{-/-}$ mice aged postnatal day 8 before seizures. (**A–C**) Nissl-staining of dentate gyrus. (**A**) Wild-type ($n = 3$), (**B**) LGI1$^{+/-}$ ($n = 3$) and (**C**) LGI1$^{-/-}$ ($n = 3$) mice. (**D–F**) Glial fibrillary acidic protein immunostaining with cresyl violet counterstaining of the hippocampus of (**D**) wild-type ($n = 3$), (**E**) LGI1$^{+/-}$ ($n = 3$) and (**F**) LGI1$^{-/-}$ ($n = 3$) mice. (**G–I**) Zinc transporter 3 (ZnT3) immunostaining with cresyl violet counterstaining of the hippocampus of (**G**) wild-type ($n = 3$), (**H**) LGI1$^{+/-}$ ($n = 3$) and (**I**) LGI1$^{-/-}$ ($n = 3$) mice. Scale bars: 300 μm (**A–B**); 40 μm (**D–I**).

are typical for patients with temporal lobe epilepsies as well as numerous animal models of hippocampal seizures (Dudek and Sutula, 2007). No such morphological modifications were present in LGI1$^{-/-}$ pups at postnatal day 8 before seizure onset, or in LGI1$^{+/-}$ and wild-type animals. Taken together, evidence for anatomical changes in the hippocampus, for a hippocampal origin of ictal activity and for strong expression of *LGI1* in the dentate gyrus and CA3 region (Herranz-Perez *et al.*, 2010) support a localization of LGI1-related epileptic activity to this region.

Heterozygous LGI1$^{+/-}$ mice: a model for ADLTE?

Since human *LGI1* mutations are linked to ADLTE, an autosomal dominant trait, we searched for epileptic behaviour in heterozygous LGI1$^{+/-}$ mice. These animals showed no evidence of spontaneous behavioural epileptic seizures at any age up to 15 months. We cannot completely exclude rare seizures, but the absence of pathological changes in hippocampal anatomy suggests that heterozygous mice did not experience recurrent subclinical seizures. However, adult LGI1$^{+/-}$ mice were more susceptible to sound-induced seizures than wild-type littermates, as are some patients with ADLTE. Audiogenic seizures possessed a comparable age dependence and similar violent behavioural manifestations, including wild running and clonic or tonic activities, to those induced in wild-type mice (Seyfried *et al.*, 1999). This susceptibility is striking, since the C57BL/6 mouse strain is normally resistant to audiogenic seizures. Our *LGI1*-deficient mice were derived from 75% C57BL/6 and 25% 129S2Sv/pas hybrid background, suggesting that *LGI1* deficiency underlies their susceptibility to audiogenic seizures. Interestingly, both *LGI1* and the *mass1* gene, mutated in the *Frings* mouse model of audiogenic epilepsy (Skradski *et al.*, 2001), share structural homology, including epilepsy-associated repeats (Scheel *et al.*, 2002).

Altogether, our findings highlight a gene dosage relation between LGI1 and epileptic syndromes. Lack of one *LGI1* copy confers an enhanced susceptibility to auditory-evoked seizures, as in some patients with ADLTE, while early onset spontaneous seizures occur in mice lacking two copies. These observations indicate that LGI1 knockout mice could provide two distinct animal models for epilepsy: heterozygous mice recapitulate the genetic cause and mimic the human condition with an auditory epileptogenic trigger, while homozygous mice are interesting due to an early onset of spontaneous seizures with a probable origin in the temporal lobe structures. In particular, this model may be useful in studies on the temporal development of seizures and the spatial recruitment of distant brain structures as well as the electrical characterization of the transition to seizure or ictogenesis. Our results confirm genetic evidence that *LGI1* haploinsufficiency can lead to seizures. The LGI1 knockout mouse thus provides a novel non-lesional epileptic mouse model that may open new therapeutical avenues for

patients with pharmacoresistant epilepsies, including but not limited to those with *LGI1* mutations, by identifying new pre- and postsynaptic targets for modulation of circuit excitability by LGI1.

LGI1-deficient mouse: a tool to understand the function of LGI1

The LGI1 knockout mouse may help understand the function of this secreted neuronal protein. While the loss of both *LGI1* alleles by somatic mutations in glioma cell lines was first thought to contribute to malignant brain tumours (Chernova *et al.*, 1998), our findings emphasize a role in epileptogenesis. Since we found no evidence for gliomas in LGI1$^{-/-}$ Nissl-stained brains sections ($n = 8$), the germinal loss of LGI1 seems unlikely to be related to brain tumour genesis. While tumours might conceivably develop in LGI1$^{-/-}$ mice if they did not die prematurely, there is no evidence for an elevated rate of malignancy in families with ADLTE (Brodtkorb *et al.*, 2003).

Recent data have shown that LGI1 shapes neuronal morphology at multiple levels. It forms part of canonical pathways controlling axon guidance (Kunapuli *et al.*, 2009), hippocampal neurite outgrowth *in vitro* (Owuor *et al.*, 2009) and postnatal pruning of granule cell dendrites and glutamatergic synapses (Zhou *et al.*, 2009). Possibly developmental actions of LGI1 on dendritic and synaptic maturation contribute to epileptogenesis. We detected no major anomalies in cortical lamination in either LGI1$^{-/-}$ or LGI1$^{+/-}$ mice, but further work is needed to define more subtle morphological changes.

We consistently observed that recurrent seizures were first initiated at postnatal day 10 in LGI1$^{-/-}$ mice. This date of onset was not correlated with the developmental pattern of LGI1 expression. In the wild-type mouse, the antibody we used (ab30868; specificity proven, since there was no LGI1 signal in tissue from knockout mice) detected LGI1 as early as embryonic day 16, somewhat earlier than previous studies (Furlan *et al.*, 2006; Ribeiro *et al.*, 2008; Zhou *et al.*, 2009). This onset timing of seizures, loss of body weight and premature death in LGI1$^{-/-}$ mice mirrors that in *SCN1A* knockout and knock-in mice, which are models for severe myoclonic epilepsy of infancy (Yu *et al.*, 2006; Ogiwara *et al.*, 2007). Many significant developmental events occur in rodents during the restricted time window when seizures emerge in LGI1$^{-/-}$ mice, including the switch in polarity of GABAergic signalling in inhibitory interneurons (Ben-Ari and Holmes, 2006) and the maturation of excitatory synapses terminating on principal cells of the cortex and hippocampus (Zhou *et al.*, 2009).

Recent reports converge to show that LGI1 regulates the development of glutamatergic synapses (Fukata *et al.*, 2010; Yu *et al.*, 2010) and yet contradict each other. Yu *et al*. (2010) suggest that an absence of LGI1 enhances excitatory synaptic transmission with an increased frequency of excitatory postsynaptic synaptic currents but no difference in their amplitude (Yu *et al.*, 2010). In contrast, Fukata and colleagues (2010) found a reduction in the amplitude of excitatory postsynaptic synaptic currents (selectively of AMPA-mediated excitatory postsynaptic synaptic currents), but no change in their frequency (Fukata *et al.*, 2010). Further studies may reveal the reasons for this difference.

It remains unclear how mutations in or inactivation of LGI1 led to epilepsy. Possibly, temporally restricted deletion of LGI1 using inducible Cre transgenic mice may permit the differentiation of defects in synaptic transmission and/or cellular excitability due to prenatal or postnatal neuronal development, and those due to a lack of LGI1 in the adult. *LGI1* is a novel type of epilepsy gene, structurally distinct from ion channel genes involved in other inherited epilepsies. The human ADLTE syndrome may therefore depend on a pathway to enhanced brain excitability different from those resulting from altered ion channels.

Acknowledgements

The mouse mutant line was established at the Mouse Clinical Institute—Institut Clinique de la Souris (Illkirch, France). We would like to thank Jerome Garrigue for genotyping, Annick Prigent for immunohistochemistry, Philippe Couarch for technical help and Isabelle Gourfinkel-An and Stéphanie Millecamps for helpful discussion. We are also grateful to Revital Rattenbach for kindly providing the *PGK*-Cre mouse line and Richard Palmiter for offering the anti-ZnT3 antibody.

Funding

Fondation pour la Recherche sur le Cerveau (FRC); FP6 Integrated Project EPICURE; Sanofi-Aventis; Japan Society of the Promotion of Sciences (to S.B.); Ile de France (to E.C.); Contrat d'interface INSERM (to V.N.) and Agence Nationale de la Recherche (ANR-08-MNP-013 to C.D.). Funding to pay the Open Access publication charges for this article was provided by Fondation pour la Rechercher Medicale.

Supplementary material

Supplementary material is available at *Brain* online.

References

Baulac S, Baulac M. Advances on the genetics of mendelian idiopathic epilepsies. Neurol Clin 2009; 27: 1041–61.

Ben-Ari Y, Holmes GL. Effects of seizures on developmental processes in the immature brain. Lancet Neurol 2006; 5: 1055–63.

Brodtkorb E, Nakken KO, Steinlein OK. No evidence for a seriously increased malignancy risk in LGI1-caused epilepsy. Epilepsy Res 2003; 56: 205–8.

Chabrol E, Popescu C, Gourfinkel-An I, Trouillard O, Depienne C, Senechal K, et al. Two novel epilepsy-linked mutations leading to a loss of function of LGI1. Arch Neurol 2007; 64: 217–22.

Chernova OB, Somerville RP, Cowell JK. A novel gene, LGI1, from 10q24 is rearranged and downregulated in malignant brain tumors. Oncogene 1998; 17: 2873–81.

de Bellescize J, Boutry N, Chabrol E, Andre-Obadia N, Arzimanoglou A, Leguern E, et al. A novel three base-pair LGI1 deletion leading to loss of function in a family with autosomal dominant lateral temporal epilepsy and migraine-like episodes. Epilepsy Res 2009; 85: 118–22.

Di Bonaventura C, Carni M, Diani E, Fattouch J, Vaudano EA, Egeo G, et al. Drug resistant ADLTE and recurrent partial status epilepticus with dysphasic features in a family with a novel LGI1 mutation: electroclinical, genetic, and EEG/fMRI findings. Epilepsia 2009; 50: 2481–6.

Dudek FE, Sutula TP. Epileptogenesis in the dentate gyrus: a critical perspective. Prog Brain Res 2007; 163: 755–73.

Fukata Y, Adesnik H, Iwanaga T, Bredt DS, Nicoll RA, Fukata M. Epilepsy-related ligand/receptor complex LGI1 and ADAM22 regulate synaptic transmission. Science 2006; 313: 1792–5.

Fukata Y, Lovero KL, Iwanaga T, Watanabe A, Yokoi N, Tabuchi K, et al. Disruption of LGI1-linked synaptic complex causes abnormal synaptic transmission and epilepsy. Proc Natl Acad Sci USA 2010; 107: 3799–804.

Furlan S, Roncaroli F, Forner F, Vitiello L, Calabria E, Piquer-Sirerol S, et al. The LGI1/epitempin gene encodes two protein isoforms differentially expressed in human brain. J Neurochem 2006; 98: 985–91.

Head K, Gong S, Joseph S, Wang C, Burkhardt T, Rossi MR, et al. Defining the expression pattern of the LGI1 gene in BAC transgenic mice. Mamm Genome 2007; 18: 328–37.

Herranz-Perez V, Olucha-Bordonau FE, Morante-Redolat JM, Perez-Tur J. Regional distribution of the leucine-rich glioma inactivated (LGI) gene family transcripts in the adult mouse brain. Brain Res 2010; 1307: 177–94.

Kalachikov S, Evgrafov O, Ross B, Winawer M, Barker-Cummings C, Martinelli Boneschi F, et al. Mutations in LGI1 cause autosomal-dominant partial epilepsy with auditory features. Nat Genet 2002; 30: 335–41.

Kunapuli P, Jang GF, Kazim L, Cowell JK. Mass spectrometry identifies LGI1-interacting proteins that are involved in synaptic vesicle function in the human brain. J Mol Neurosci 2009; 39: 137–43.

Lallemand Y, Luria V, Haffner-Krausz R, Lonai P. Maternally expressed PGK-Cre transgene as a tool for early and uniform activation of the Cre site-specific recombinase. Transgenic Res 1998; 7: 105–12.

Michelucci R, Pasini E, Nobile C. Lateral temporal lobe epilepsies: clinical and genetic features. Epilepsia 2009; 50 (Suppl 5): 52–4.

Morante-Redolat JM, Gorostidi-Pagola A, Piquer-Sirerol S, Saenz A, Poza JJ, Galan J, et al. Mutations in the LGI1/Epitempin gene on 10q24 cause autosomal dominant lateral temporal epilepsy. Hum Mol Genet 2002; 11: 1119–28.

Navarro V, Martinerie J, Le Van Quyen M, Clemenceau S, Adam C, Baulac M, et al. Seizure anticipation in human neocortical partial epilepsy. Brain 2002; 125: 640–55.

Nobile C, Michelucci R, Andreazza S, Pasini E, Tosatto SC, Striano P. LGI1 mutations in autosomal dominant and sporadic lateral temporal epilepsy. Hum Mutat 2009; 30: 530–6.

Ogiwara I, Miyamoto H, Morita N, Atapour N, Mazaki E, Inoue I, et al. Na(v)1.1 localizes to axons of parvalbumin-positive inhibitory interneurons: a circuit basis for epileptic seizures in mice carrying an Scn1a gene mutation. J Neurosci 2007; 27: 5903–14.

Ottman R, Winawer MR, Kalachikov S, Barker-Cummings C, Gilliam TC, Pedley TA, et al. LGI1 mutations in autosomal dominant partial epilepsy with auditory features. Neurology 2004; 62: 1120–6.

Owuor K, Harel NY, Englot DJ, Hisama F, Blumenfeld H, Strittmatter SM. LGI1-associated epilepsy through altered ADAM23-dependent neuronal morphology. Mol Cell Neurosci 2009; 42: 44857.

Palmiter RD, Cole TB, Quaife CJ, Findley SD. ZnT-3, a putative transporter of zinc into synaptic vesicles. Proc Natl Acad Sci USA 1996; 93: 14934–9.

Poza JJ, Saenz A, Martinez-Gil A, Cheron N, Cobo AM, Urtasun M, et al. Autosomal dominant lateral temporal epilepsy: clinical and genetic study of a large Basque pedigree linked to chromosome 10q. Ann Neurol 1999; 45: 182–8.

Ribeiro PA, Sbragia L, Gilioli R, Langone F, Conte FF, Lopes-Cendes I. Expression profile of lgi1 gene in mouse brain during development. J Mol Neurosci 2008; 35: 323–9.

Sagane K, Ishihama Y, Sugimoto H. LGI1 and LGI4 bind to ADAM22, ADAM23 and ADAM11. Int J Biol Sci 2008; 4: 387–96.

Scheel H, Tomiuk S, Hofmann K. A common protein interaction domain links two recently identified epilepsy genes. Hum Mol Genet 2002; 11: 1757–62.

Schmued LC, Stowers CC, Scallet AC, Xu L. Fluoro-Jade C results in ultra high resolution and contrast labeling of degenerating neurons. Brain Res 2005; 1035: 24–31.

Schulte U, Thumfart JO, Klocker N, Sailer CA, Bildl W, Biniossek M, et al. The epilepsy-linked Lgi1 protein assembles into presynaptic Kv1 channels and inhibits inactivation by Kvbeta1. Neuron 2006; 49: 697–706.

Senechal KR, Thaller C, Noebels JL. ADPEAF mutations reduce levels of secreted LGI1, a putative tumor suppressor protein linked to epilepsy. Hum Mol Genet 2005; 14: 1613–20.

Seyfried TN, Todorova MT, Poderycki MJ. Experimental models of multifactorial epilepsies: the EL mouse and mice susceptible to audiogenic seizures. Adv Neurol 1999; 79: 279–90.

Sirerol-Piquer MS, Ayerdi-Izquierdo A, Morante-Redolat JM, Herranz-Perez V, Favell K, Barker PA, et al. The epilepsy gene LGI1 encodes a secreted glycoprotein that binds to the cell surface. Hum Mol Genet 2006; 15: 3436–45.

Skradski SL, Clark AM, Jiang H, White HS, Fu YH, Ptacek LJ. A novel gene causing a mendelian audiogenic mouse epilepsy. Neuron 2001; 31: 537–44.

Striano P, de Falco A, Diani E, Bovo G, Furlan S, Vitiello L, et al. A novel loss-of-function LGI1 mutation linked to autosomal dominant lateral temporal epilepsy. Arch Neurol 2008; 65: 939–42.

Winawer MR, Martinelli Boneschi F, Barker-Cummings C, Lee JH, Liu J, Mekios C, et al. Four new families with autosomal dominant partial epilepsy with auditory features: clinical description and linkage to chromosome 10q24. Epilepsia 2002; 43: 60–7.

Winawer MR, Ottman R, Hauser WA, Pedley TA. Autosomal dominant partial epilepsy with auditory features: defining the phenotype. Neurology 2000; 54: 2173–6.

Yagi H, Takamura Y, Yoneda T, Konno D, Akagi Y, Yoshida K, et al. Vlgr1 knockout mice show audiogenic seizure susceptibility. J Neurochem 2005; 92: 191–202.

Yu FH, Mantegazza M, Westenbroek RE, Robbins CA, Kalume F, Burton KA, et al. Reduced sodium current in GABAergic interneurons in a mouse model of severe myoclonic epilepsy in infancy. Nat Neurosci 2006; 9: 1142–9.

Yu YE, Wen L, Silva J, Li Z, Head K, Sossey-Alaoui K, et al. Lgi1 null mutant mice exhibit myoclonic seizures and CA1 neuronal hyperexcitability. Hum Mol Genet 2010; 19: 1702–11.

Zhou YD, Lee S, Jin Z, Wright M, Smith SE, Anderson MP. Arrested maturation of excitatory synapses in autosomal dominant lateral temporal lobe epilepsy. Nat Med 2009; 15: 1208–14.